LASER-RESPONSIVE SHAPE MEMORY POLYMER

By

RAO FEI

A THESIS PRESENTED TO THE GRADUATE SCHOOL
OF THE UNIVERSITY OF FLORIDA IN PARTIAL FULFILLMENT
OF THE REQUIREMENTS FOR THE DEGREE OF
MASTER OF SCIENCE

UNIVERSITY OF FLORIDA

2017

ACKNOWLEDGMENTS

I would like to acknowledge my advisor Dr. Peng Jiang, for his advisement and guidance throughout this research. I must also acknowledge the other of my committee, Dr. Kirk J. Ziegler, for his valuable advice to the work. Besides, I would like to thank Sin-Yen Leo for the work on scanning electron microscopy, Yifan Zhang for the work on atomic force microscopy, and Yongliang Ni and Zhuxiao Gu for their concern and help in lab. Finally, I would like to thank all mentioned above again for the support during my study and experiments, as well as my parents and friends.

TABLE OF CONTENTS

page

LIST OF FIGURES

Figure page

Abstract of Thesis Presented to the Graduate School
of the University of Florida in Partial Fulfillment of the
Requirements for the Degree of Master of Science

LASER-RESPONSIVE SHAPE MEMORY POLYMER

By

Rao Fei

December 2017

Chair: Peng Jiang
Major: Chemical Engineering

Shape memory effect has been widely studied for applications in different areas since discovered. However, the development of shape memory polymers has been focusing on the function of whole bulk polymer, regardless of the advantages of faster response and practical uses in smaller scale.

Based on a vapor induced surface-reactive shape memory polymer, a laser-responsive spot-reactive shape memory effect is developed, by cooperating the polymer with graphene oxide as the light absorber. The shape memory effect shows a significant color change, as the macroporous structure changes from disordered to highly ordered, driven by the movements of graphene oxide. This laser-responsive localized shape memory effect is proved to be reversible, and could have a promising prospect for its application.

CHAPTER 1
INTRODUCTION

1.1 Shape Memory Polymers with Nanocomposites

1.1.1 General Shape Memory Polymers

Shape memory polymers are an emerging class of active polymers that have the capability to change among their permanent shapes and temporary configurations under external stimulus.[1-3]

Since the 1980s, shape memory polymers have been widely researched. The shape memory effect is a result from a combination of polymer morphology and specific processing, which can be understood as a polymer functionalization. Generally shape memory polymers have the unique advantages of being lightweight and inexpensive and of having low density, good manufacturability, high shape deformability, and an easily tailorable glass transition temperature compared with shape memory alloys or ceramics. They also have some drawbacks, such as low deformation stiffness and low recovery stress. Due to their unique properties and development potential, shape memory polymers have become a hot area in various industries and researches.[1,4,5]

1.1.2 General Mechanism of Shape Memory Effect

The shape memory research was in initially founded on the thermally induced dual-shape effect.[4] The thermally induced shape memory effect involves polymers whose chain mobility is very dependent on temperature (Figure 1-1). The polymer chains have a “permanent” structure which is thermally stable. They can be deformed under some certain methods, but when heated to their glass transition temperatures, as the mobility of chains increases, the polymers tend to recover to the “permanent” shapes.

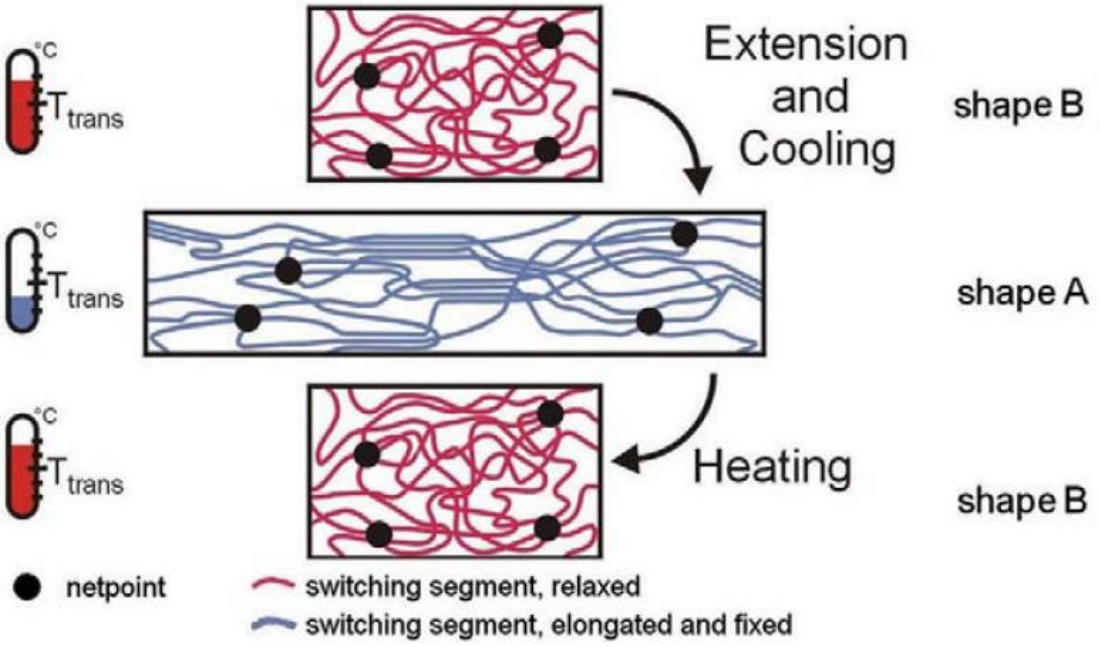

Figure 1-1. Molecular mechanism of the thermally induced shape memory effect.[4]

Shape memory polymers responding to stimulus other than heat, such as light, electric, magnetic field, and vapor, are then developed, as we human have much higher degree of control of them on a piece of polymer in most cases.[1]

1.1.3 Light-responsive Shape Memory Effect

Among the stimulus we have ever discovered, light, of which we can easily control the intensity, wave length, place to shine on, and even polarization conditions, is one of the best choices.

Based on the recovery mechanism, current light-responsive shape memory polymers can be categorized into two types. One is known as the photochemical shape memory polymers, which are involved in chemical reactions of the polymer chains with photons, thus they usually need to interact with light with a specific wavelength (mostly violet or ultraviolet) for the material programming. So far the chemical reactions within the polymer is inconvenient for us to utilize, as a result, this type is less reported and applied. [6,7,8] The other type is understood as

indirect actuation of the thermal-induced shape memory effect. Many published works in this area use infrared or near-infrared light source, as infrared light has more significant thermal effect.[4,9,10] This kind of shape memory polymers are usually fabricated by incorporating light absorbers such as carbon nanotubes [9,11], gold nanoparticles [12], and graphene [10]. Those light absorbers are considered to absorb energy of light in a range of wavelength, to increase the temperature of polymer, thus increasing the movements of polymer chains to recovery. In addition to the higher controllability, light for indirect heating is considered safer than the direct, electrical, and magnetic heating.

Published works have demonstrated many different ideas on functionalization of the light-responsive shape memory polymers, such as differential shrinking [13] and self-healing [14]. However, as the same case of shape memory polymers under other stimulus, present works all focus on the shape change or functionalization of the whole bulk material, wasting the potential of light with localized reactions. Therefore, in this work, my goal is to realize a fast-responsive and localized shape memory effect responding to light, which could have promising prospect in fabrications.

1.2 Graphene Oxide

Since first published in 2004, graphene, the single layer of sp^2-bonded carbon atoms, has attracted great attention in researches due to its unique mechanical, electrical, thermal and optical properties.[15] However, some of the properties such as hydrophobicity, along with the expensiveness in fabrication, have always been issues for its applications.

On the other hand, as the precursor of graphene, graphene oxide has much higher solubilities in many common solvents, similar properties, and cheaper price.[16] The molecular structure of graphene oxide is very similar to graphene, especially for the edge-oxidized ones, and this makes them similar in thermal and optical properties. In addition, the oxygenated

functional groups could lower the surface energy, which helps to better disperse in some solvents.[18] Among the common used light absorbers (carbon nanotubes, gold nanoparticles, graphene nanosheets), graphene oxide has good absorbance crossing all wavelengths of light, meanwhile it is easy to modify the size and the functional groups of graphene oxide. Therefore in this work I choose graphene oxide as the light absorber.

In the same case as other light absorbers, the detailed mechanism of the shape memory effect involving graphene oxide is not strictly studied yet. The role of light absorber has been long considered as either photochemical reactants, or light-heat exchanger [4], but recently some work could reveal another physical role for them. In Thakur's publication, it was graphene oxide that directly increased the Brownian movements rather than heat (Figure 1-2).[14]

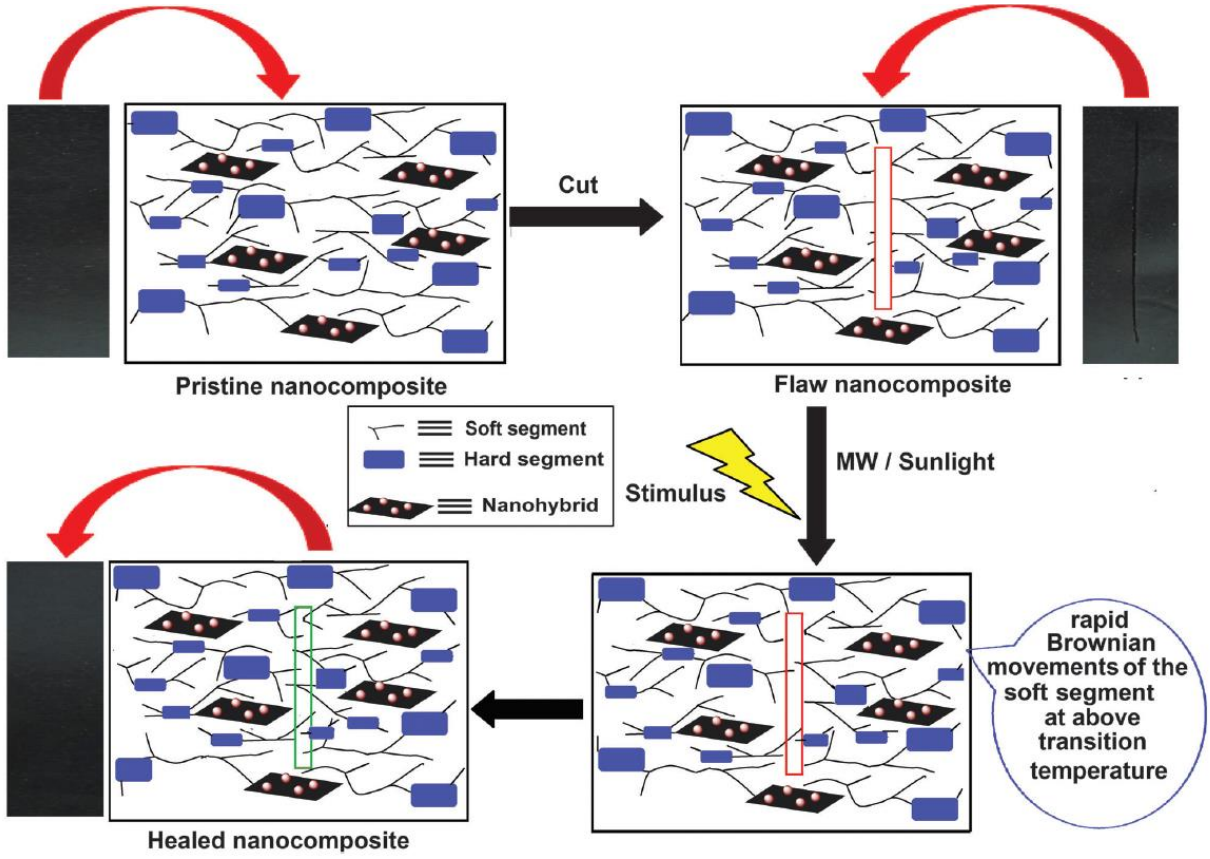

Figure 1-2. Thakur's mechanism for the self-healing, where graphene oxide nanocomposites directly perform work instead of heating. [14]

1.3 Synthesis

1.3.1 Choice of Shape Memory Polymer

The macroporous photonic crystal shape memory polymer synthesized from ethoxylated (20) trimethylolpropane triacrylate (SR415) and polyethylene glycol (600) diacrylate (SR610) was first reported by Fang in 2015.[3] It had great advantages on fast response speed and cold programming. Further, the functionalization of the polymer only exists at its surface, which means the function could be realized at a much smaller scale. These aspects are necessary to realize the fast-responsive localized shape memory with practical use, so I choose this polymer as well as similar synthesis methods to firstly realize the goal.

1.3.2 Synthesis of Graphene Oxide

Due to the importance of graphene oxide as the precursor of graphene, its synthesis methods have been well-established for long. Reacting graphite with strong acid (sulfuric acid) and strong oxidant (potassium permanganate), known as Hummers' method, is a very common method to obtain graphene oxide with single atomic layer.[16,17] In this method, the sp^2 bonding of carbon atoms will not be disrupted, so some electronic properties as well as optical properties will remain similar to graphene.

1.3.3 Synthesis of 3D Highly Ordered Silica Spheres

The Stöber method is a commonly used chemical process to prepare silica nanoparticles with uniform size (less than 5% diameter variation) in material science. During a Stöber process, tetraethyl orthosilicate ($Si(OEt)_4$) is hydrolyzed in the mixture of water and ethanol, then the produced ethoxysilanols condense with each other to form larger molecules, and the diameter of silica particles can be strictly controlled by reactant concentrations, catalysts, and temperature.[19]

The convective self-assembly method technology developed by Jiang [20] could be used to crystalize the synthesized silica spheres into 3D highly ordered structure. In this way, particles

with uniform size could be assembled on the substrate in the hexagonal closest packed structure, and the substrate could then be used as a template to synthesize products with highly ordered porous structure.

CHAPTER 2
EXPERIMENTAL SECTION

2.1 Fabrication of Graphene Oxide

Graphene oxide was prepared using Hummers' method.[15] In each batch of synthesis, 0.5 g graphite (natural, briquetting grade, -100 mesh, Alfa Aesar) was dispersed in 50 mL concentrated sulfuric acid (A144-212, Fisher Scientific) and stirred for 30 min, then cooled to 0℃ in an ice bath. 1.2 g $KMnO_4$ (Certified ACS, Fisher Chemical) was then slowly added to the mixture, and stirred at 25℃ for 60 min. The temperature was then elevated to 70℃ and remained for another hour. After reaction, the mixture was poured into 500 mL water with 3 mL H_2O_2 (H325-500, Certified ACS 30%, Fisher Chemical). The dispersions were centrifuged and washed by equal volume of deionized water for 6 times, and then dried out at 80℃ at atmospheric pressure.

2.2 Fabrication of Laser-responsive Shape Memory Polymer Membranes

As is mentioned in the introduction, the synthesis of shape memory polymer is following the method of Fang.[3] First, the synthesis of monodisperse silica microspheres was performed following the Stöber method.[19] The synthesized silica microspheres were purified in 200-proof ethanol by 6 times of centrifugation and dispersion cycles. The purified silica particles were then assembled on glass microslides using the convective self-assembly technology.[20] The glass slide with silica colloidal crystal on its surface was covered by another microslide, separated by adhesive spacer with thickness of 2.0 mm, to form the template for desired shape memory polymer. Next, the interstitials in-between the assembled silica microspheres were filled up with the mixture consisting of ethoxylated (20) trimethylolpropane triacrylate (SR415, Sartomer), polyethylene glycol (600) diacrylate (SR610, Sartomer), synthesized graphene oxide, and Darocur 1173 (2-hydroxy-2-methyl-1-phenyl-1-propanone, BASF) as the photoinitiator. The

ratio of SR610 and SR415 was in the range from 1:1 to 6:1, the concentration of photoinitiator was fixed at 1 wt%, and the concentration of graphene oxide was in the range from 0.2% to 1.6%. The monomer mixture was photopolymerized in a pulsed UV curing system (RC 742, Xenon) for totally 24 seconds. Between each run as 4 s, the sample was taken out for cooling for 10 s, and was flipped to the other side facing the lamp. The polymerized membrane was cut off from the glass slide and soaked in a 2 vol% hydrofluoric acid aqueous solution for 5 min and finally rinsed with deionized water.

2.3 Sample Characterization

2.3.1 Atomic Force Microscopy (AFM)

Amplitude-modulation atomic force microscopy was performed on an MFP-3D AFM (Asylum Research, Inc.) with a PPP-NCHR probe (tip radius < 10 nm) as the sensor. The scan mode was set as AC mode, with scan rate of 1 Hz, scan point of 128, and scan lines of 128, for both shape memory samples and graphene oxide.

2.3.2 Scanning Electron Microscopy (SEM)

The scanning electron microscopy images were performed on an FEI XL-40 FEG-SEM, with parameter HV=7.00 kV for deformed sample, and HV=5.00kV for recovered sample. In this case, the magnification was 14000 times, and other parameters were mode=SE, curr=0.18 nA, WD=6.2 mm, and det=TLD for both kinds of samples. The sample was cut to expose the boundary between porous and non-porous part in cross section, and a gold layer with thickness of 15 nm was sputtered onto the sample for imaging.

2.3.3 Optical Reflection Spectra

Normal-incidence optical reflection spectra were obtained on Ocean Optics HR4000 high-resolution vis-NIR spectrometer with the R600-7 reflection probe and a tungsten halogen light source (LS-1). The maximum reflectivity was obtained from the reflection of an aluminum-

sputtered (1000 nm thick) silicon wafer, and zero reflex condition was measured when all the light was reflected out by a wafer set as 45 °to the ground.

2.3.4 Laser Recovery

The laser recovery of the shape memory polymers were performed using a 30mW handheld green laser pointer (SKY 30mW handheld 515 nm focusable laser pointer with dual lock), during which sunglasses are used for eyes' protection. The shape memory polymers could be recovered by lasers in other wavelengths as well, but only green laser recovered samples are involved as data in this article.

CHAPTER 3
RESULTS AND DISCUSSION

3.1 General Tests

Photographs showing the general looks of the synthesized macroporous shape memory polymer membrane are below (Figure 3-1). The polymer can be deformed under water to become totally dark without any other external stimulus (Figure 3-1a). Similar to Fang's result [3], the polymer could be recovered by vapor of acetone (Figure 3-1b,c), and it seems much shinier than Fang's sample as the background is black. In addition, the sample can be recovered by irradiation of laser within 2 seconds (Figure 3-1d), which successfully achieves the goal of localized control. The deformation and recovery by laser could be repeated on the same spot of a sample for over 10 times without significant changes (more details in 3.4 Results of Optical Reflection Spectra).

The thermal recovery is however not observed. After heating on a glass substrate in an oven with the temperature from 40℃ to 110℃ for 10 min, the shape memory polymers do not show any apparent change. Temperature higher than 120℃ would cause the inactivity of the shape memory effect, which means the polymer can no longer be recovered. Similarly, after irradiation on the recovered sample for 10 s, the polymer starts to carbonization. These facts strongly suggest that graphene oxide plays a role different from heating the material. A possible explanation could be that the Brownian movements induced by light perform work directly to recover the polymer structure, and this effect is more significant in the laser recovery than that induced by heat while they both exist.

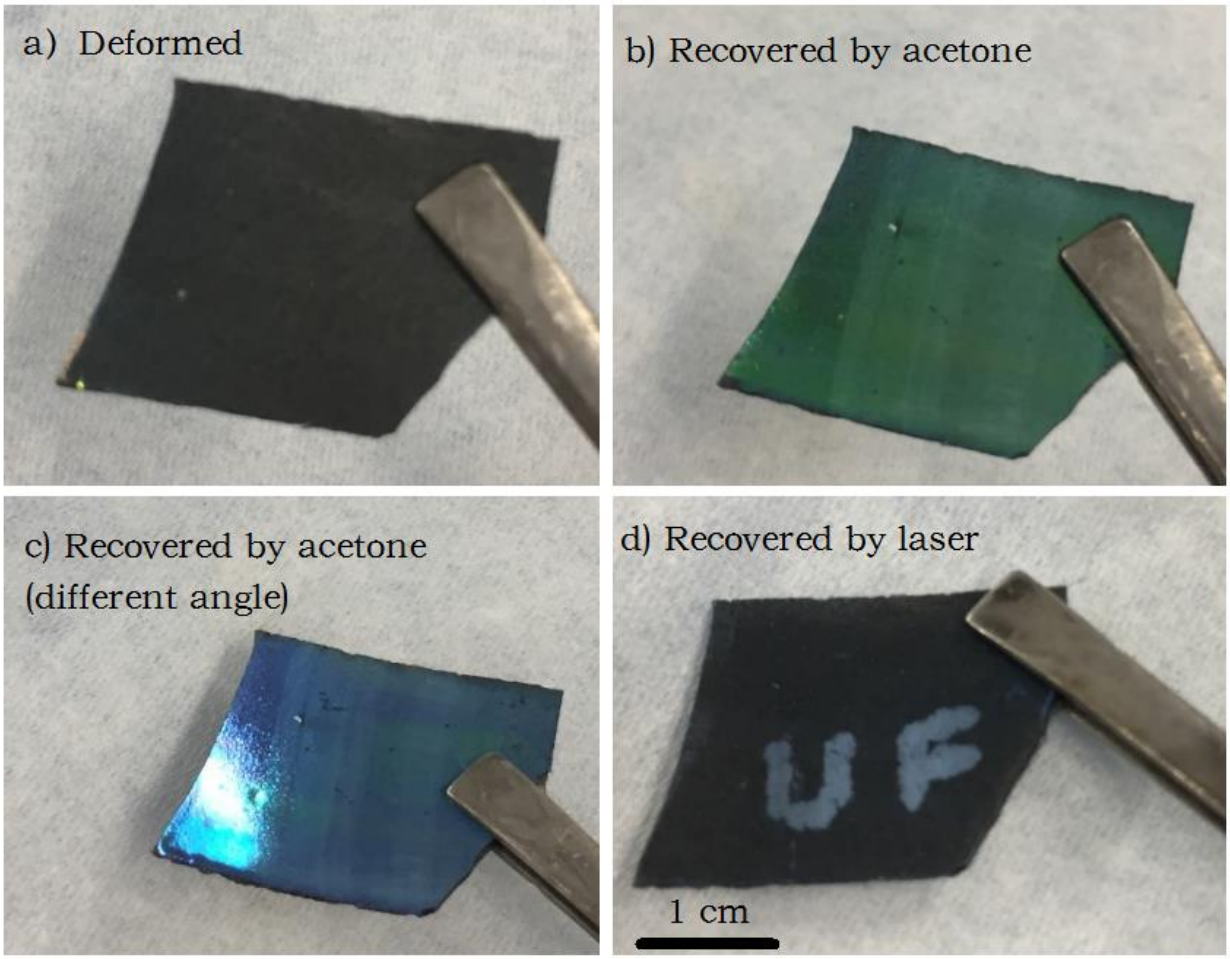

Figure 3-3. Photographs of same polymer membrane after a) deformation under water. b) & c) exposing to acetone vapor. d) recovered by laser irradiation.

Among all the ratios of SR610 to SR415 from 1:1 to 6:1, the 6:1 ratio gives the best result on shininess of recovery. The ratio of two monomers is then fixed as 6:1, to test the proper concentrations of graphene oxide. In the shape memory effect, graphene oxide is supposed to absorb light and transfer the energy for recovery, so the goal is to achieve the highest possible concentration of graphene oxide. The fact is that concentrations higher than 1.3% would make the monomers very difficult to polymerize, as most energy of UV is absorbed by graphene oxide. One way to increase the limit is to make thinner membrane by decreasing the thickness of spacer,

but considering the practical uses of the polymer this way is not tried. The concentration is finally fixed as 1.1% for the spacer thickness of 2.0 mm.

Photographs of the laser recovery of a sample with finally fixed ratio and concentration are shown below (Figure 3-2).

Figure 3-2. Photographs of laser recovery of polymer membrane with ratio of SR610:SR415=6:1, and 1.1% concentration of graphene oxide a) before the irradiation. b) during the irradiation. c) after the irradiation by the green laser.

3.2 Results of AFM

3.2.1 AFM of Graphene Oxide

Following graphs from AFM roughly shows the thickness and sizes of the graphene oxide sheets (Figure 3-3). The small pieces of graphene oxide has the size around 100 nm (Figure 3-3c,d), which agrees with the synthesis method.[15,21] An example of the largest piece of graphene oxide has the size around 7 μm (Figure 3-3a,b), which could be a proof of crystallization during the drying of graphene oxide.

As Fang's work [3] illustrates (also see 3.3 Results of SEM), the pore size within my synthesized polymer should be around 280 nm, and the thickness of polymer layer between pores is around 50 nm. According to the results above, some of the graphene oxide may exist in the macroporous part, and some cannot be there.

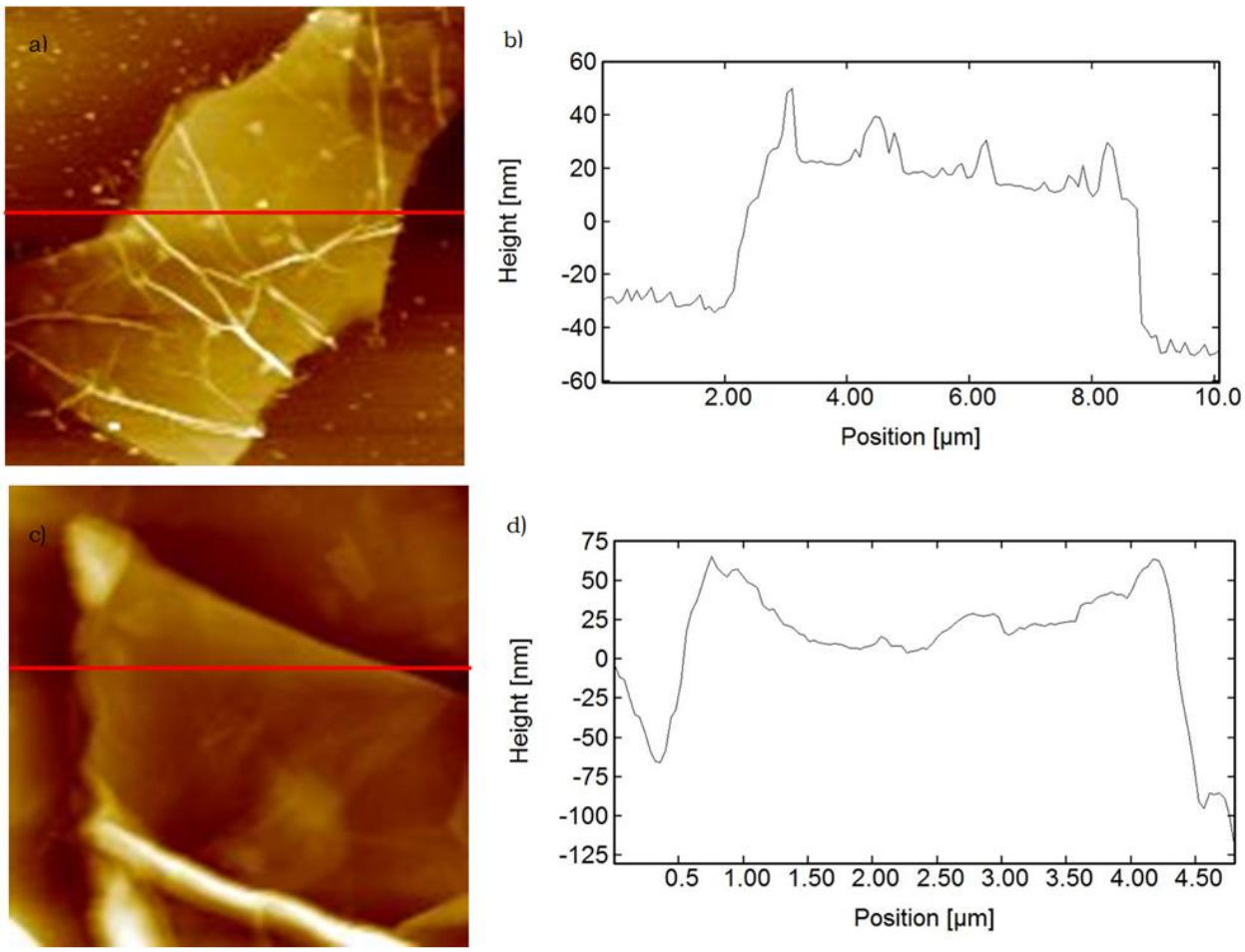

Figure 3-3. a) AFM scan of graphene oxide sheets. b) height profile for the red line in a). c) zoomed in AFM scan. d)height profile for the red line in c).

3.2.2 AFM of Shape Memory Polymer Membranes

The AFM of deformed sample (Figure 3-4) shows that the surface of dried polymer is rough. After drying out from water, the polymer shows a partly disordered structure at the surface.

In contrast, the recovered surface (Figure 3-5) is smoother, and clearly shows the ordering of the macroporous structure. Compared with Fang's works [3,22], samples with graphene oxide have more defects which can be recognized as the dark spots in Figure 3-5, and this could be due to the differential heat generated by large pieces of graphene oxide during the polymerization.

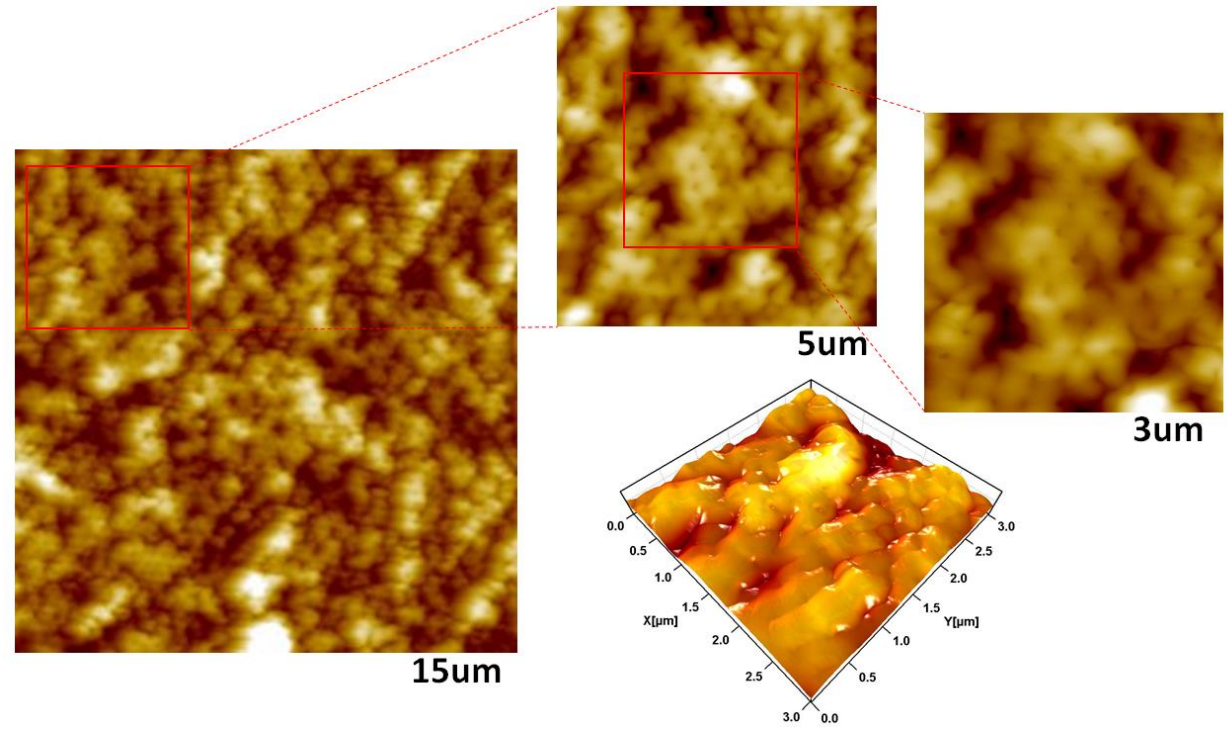

Figure 3-4. AFM scan of deformed sample surface.

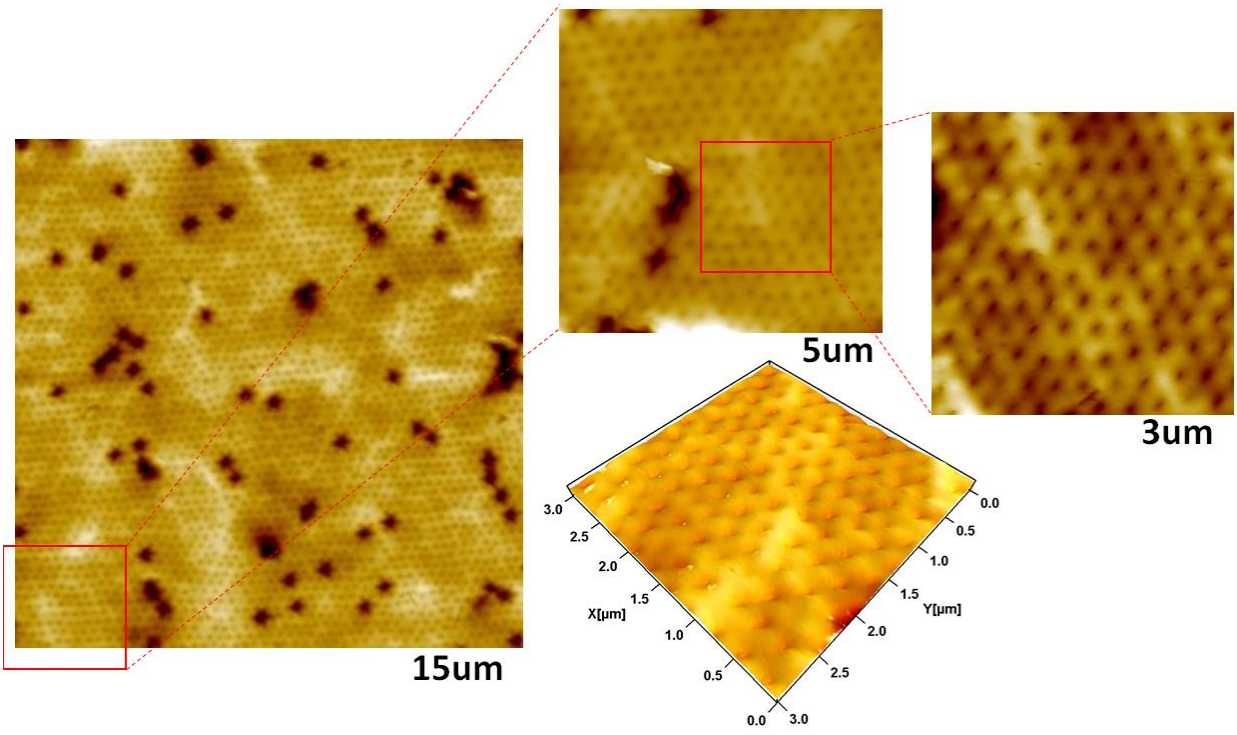

Figure 3-5. AFM scan of recovered sample surface.

3.3 Results of AFM

The cross-sectional SEM images (Figure 3-6) strongly support the conclusion from AFM images about surface roughness and ordering of pores. The image from recovered sample having the largest pore shown with diameter of around 270 nm also supports the assumed pore size.

The SEM images illustrate that by opening and closing the pores, this shape memory polymer switches its state between deformation and recovery. This agrees with the assumed mechanism of laser recovery, where rapid movements induced by graphene oxide help the pores open.

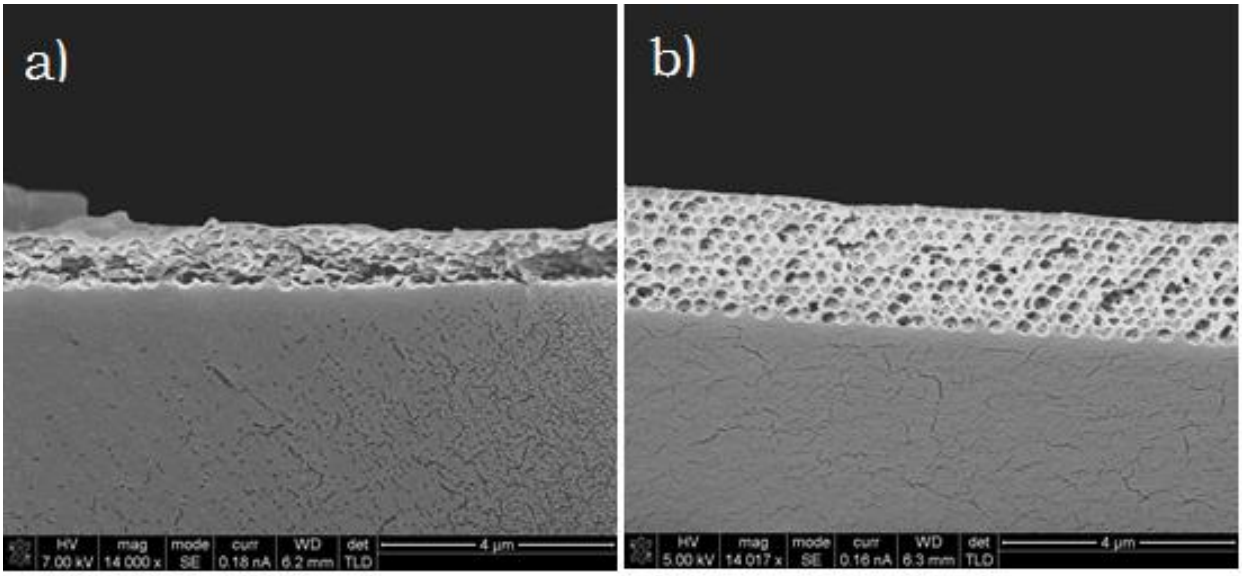

Figure 3-6. Cross-sectional SEM image of the a) deformed b) recovered sample.

3.4 Results of Optical Reflection Spectra

The reflection spectra clearly show apparent optical difference for the deformed and recovered shape memory polymer (Figure 3-7). While the deformed polymer (blue line) shows reflection just as the baseline (regulated as absolute no reflection at all wavelengths), the laser-recovered sample (black line) shows distinct reflection around 550 nm, very similar to the acetone-recovered sample (red line). High ordering quality of the pores is again confirmed by the

diffraction peaks with Fabry–Pérot fringes.[23] Compared with Fang's work [3], the blueshift of the main peak could be from the smaller pore size and change of in the ratio of two monomers.

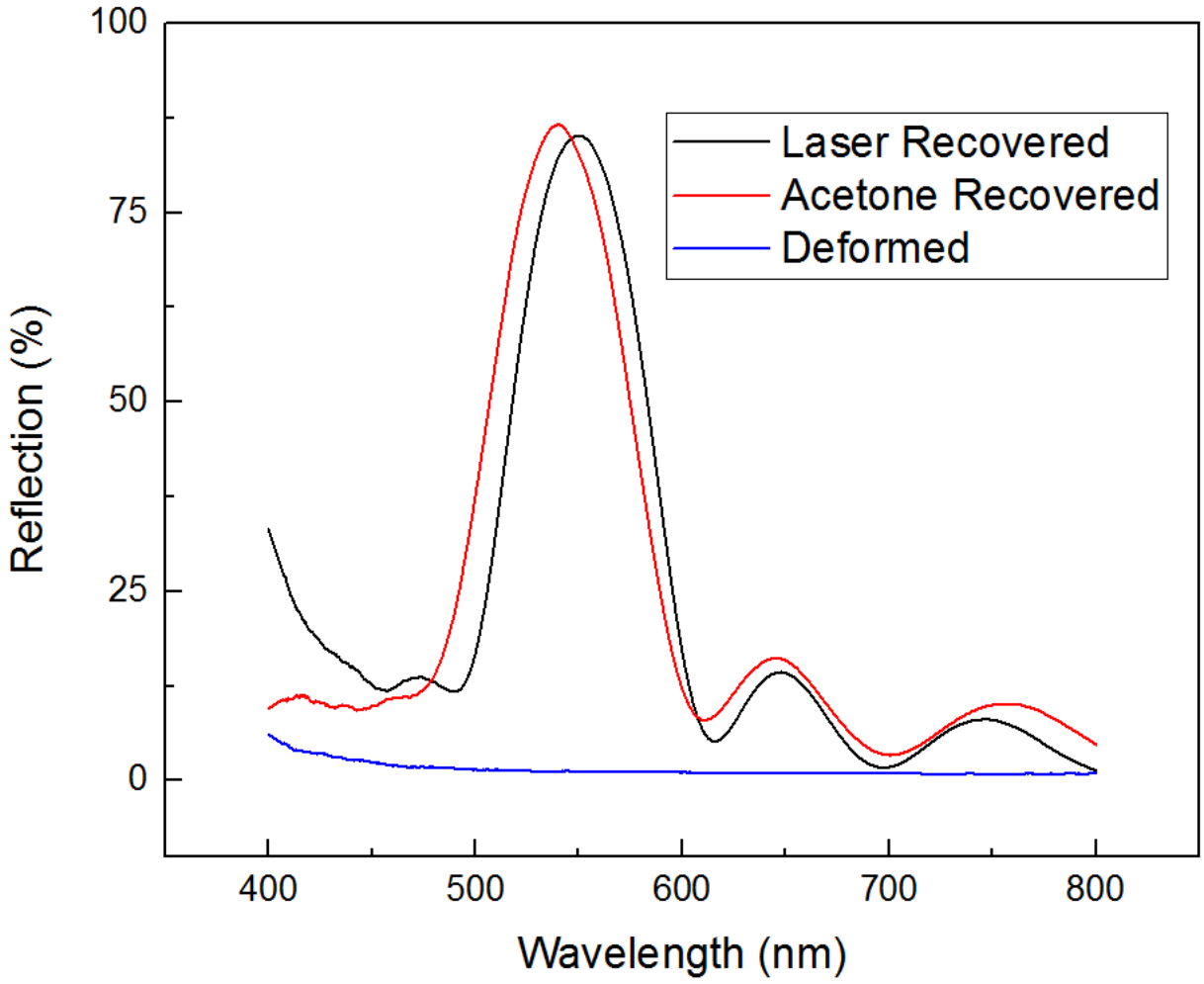

Figure 3-7. Normal-incidence optical reflection spectra comparing the same shape memory polymer recovered by laser, recovered by acetone and deformed by water.

As is mentioned earlier, this kind of shape memory effect has good reversibility and durability. Figure 3-8 shows the optical reflection spectra from the same sample cyclically recovered by laser and deformed by water. The extensive tests show that the shape memory polymer could be reused for over a hundred times without any apparent difference. However, the localized recovery could cause a tilted surface being measured, which would influence the intensity of the main peak as well as its wavelength.

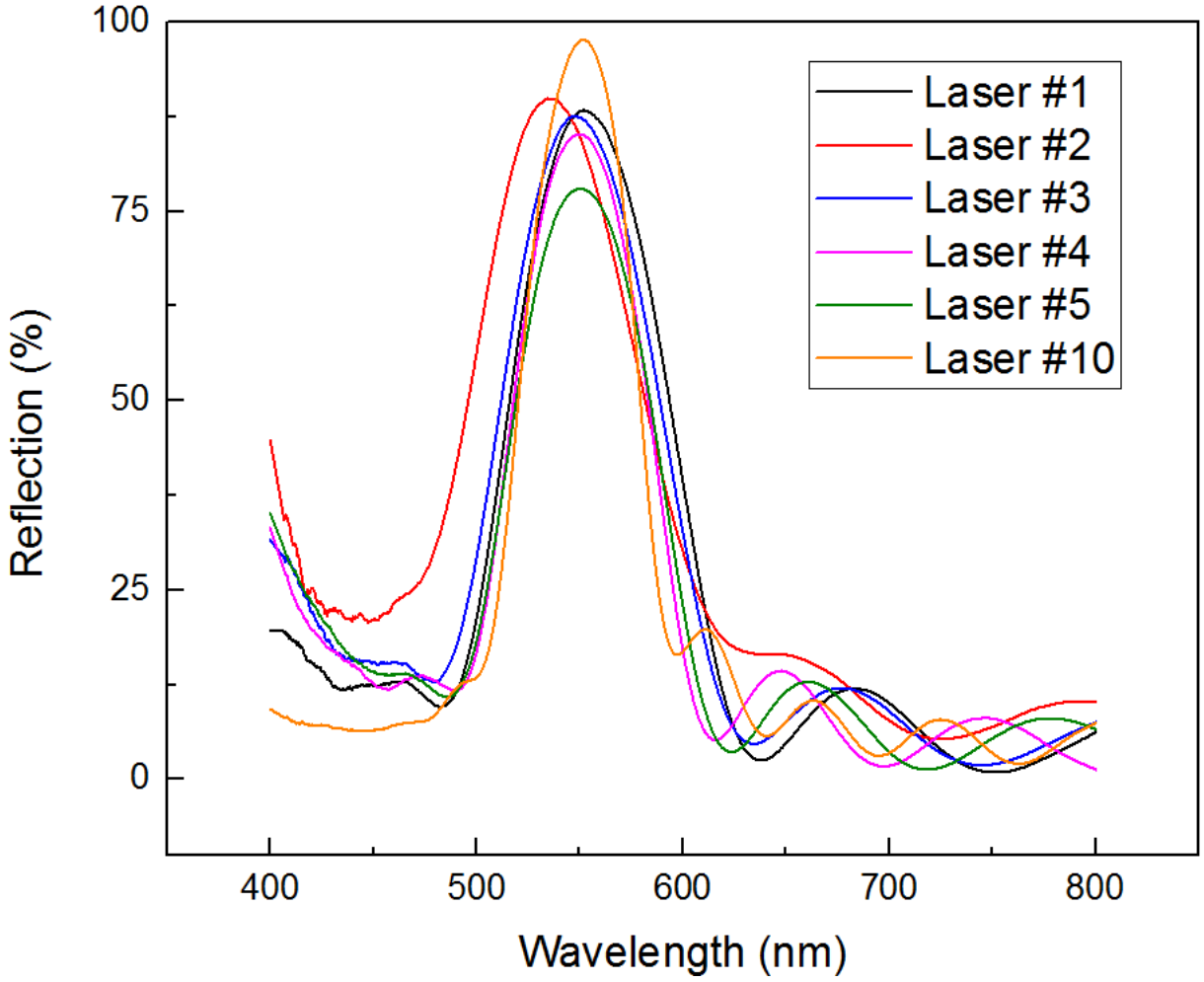

Figure 3-8. Normal-incidence optical reflection spectra from the same shape memory polymer recovered by laser for 1, 2, 3, 4, 5, and 10 times respectively.

CHAPTER 4
CONCLUSIONS

A laser-responsive shape memory polymer has been developed. The recovery of the permanent macroporous structure can be triggered by laser with power of 30 mW, and the recovery could be locally triggered at the surface spot where the laser irradiates. The striking color changing is induced by the disorder-order transitions of the porous structure, and the work performed by movements of graphene oxide is a main energy source for in the transition of states. This laser-responsive shape memory polymer is reusable, and could play important roles in different technological applications, for instance, light sensor and transducer for remote control.

LIST OF REFERENCES

1 Leng, J., Lan, X., Liu, Y., & Du, S. Shape-memory polymers and their composites: stimulus methods and applications. *Progress in Materials Science* **56**, 1077-1135 (2011)

2 Meng, H., & Li, G. A review of stimuli-responsive shape memory polymer composites. *Polymer* **54**, 2199-2221(2013).

3 Fang, Y., Ni, Y., Choi, B., Leo, S. Y., Gao, J., Ge, B., ... & Jiang, P. Chromogenic Photonic Crystals Enabled by Novel Vapor‐Responsive Shape‐Memory Polymers. *Advanced Materials* **27**, 3696-3704 (2015).

4 Behl, M., & Lendlein, A. Shape-memory polymers. *Materials today* **10**, 20-28 (2007).

5 Liu, Y., Du, H., Liu, L., & Leng, J. Shape memory polymers and their composites in aerospace applications: a review. *Smart Materials and Structures* **23**, 023001 (2014).

6 Lendlein, A., Jiang, H., Junger, O., & Langer, R. Light-induced shape-memory polymers. *Nature* **434**, 879-883 (2005).

7 Li, M. H. et al. Light-driven side-on nematic elastomer actuators. *Advanced Materials* **15**, 569–572 (2003).

8 Yu, Y., & Ikeda, T. Photodeformable polymers: A new kind of promising smart material for micro‐and nano‐applications. *Macromolecular Chemistry and Physics* **206**, 1705-1708(2005).

9 Koerner, H., Price, G., Pearce, N. A., Alexander, M., & Vaia, R. A. Remotely actuated polymer nanocomposites—stress-recovery of carbon-nanotube-filled thermoplastic elastomers. *Nature materials* **3**, 115-120 (2004).

10 Lashgari, S., Karrabi, M., Ghasemi, I., Azizi, H., Messori, M., & Paderni, K. Shape memory nanocomposite of poly (L-lactic acid)/graphene nanoplatelets triggered by infrared light and thermal heating. *Express Polymer Letters* **10**, 349 (2016).

11 Li, C., Liu, Y., Lo, C. W., & Jiang, H. Reversible white-light actuation of carbon nanotube incorporated liquid crystalline elastomer nanocomposites. *Soft Matter* **7**, 7511-7516 (2011).

12 Zhang, H., Xia, H., & Zhao, Y. Optically triggered and spatially controllable shape-memory polymer–gold nanoparticle composite materials. *Journal of Materials Chemistry* **22**, 845-849(2012).

13 Hubbard, A. M., Mailen, R. W., Zikry, M. A., Dickey, M. D., & Genzer, J. Controllable curvature from planar polymer sheets in response to light. *Soft Matter* **13**, 2299-2308(2017).

14 Thakur, S., & Karak, N. A tough, smart elastomeric bio-based hyperbranched polyurethane nanocomposite. *New Journal of Chemistry* **39**, 2146-2154 (2015).

15 Wang, Y., Shi, Z., Yu, J., Chen, L., Zhu, J., & Hu, Z. Tailoring the characteristics of graphite oxide nanosheets for the production of high-performance poly (vinyl alcohol) composites. *Carbon* **50**, 5525-5536 (2012).

16 Gambhir, S., Jalili, R., Officer, D. L., & Wallace, G. G. Chemically converted graphene: scalable chemistries to enable processing and fabrication. *NPG Asia Materials* **7**, e186 (2015).

17 Bepete, G., Anglaret, E., Ortolani, L., Morandi, V., Pénicaud, A., & Drummond, C.. Surfactant-Free single layer graphene in water. *Nature Chemistry* **9**, 347 (2016).

18 Zhu, Y., Murali, S., Cai, W., Li, X., Suk, J. W., Potts, J. R., & Ruoff, R. S. Graphene and graphene oxide: synthesis, properties, and applications. *Advanced materials* **22**, 3906-3924 (2010).

19 Stöber, W., Fink, A., & Bohn, E. Controlled growth of monodisperse silica spheres in the micron size range. *Journal of colloid and interface science* **26**, 62-69 (1968).

20 Jiang, P., Bertone, J. F., Hwang, K. S., & Colvin, V. L. Single-crystal colloidal multilayers of controlled thickness. *Chemistry of Materials* **11**, 2132-2140 (1999).

21 Edwards, R. S., & Coleman, K. S. Graphene synthesis: relationship to applications. *Nanoscale* **5**, 38-51 (2013).

22 Fang, Y., Leo, S. Y., Ni, Y., Yu, L., Qi, P., Wang, B., et al & Jiang, P. Optically bistable macroporous photonic crystals enabled by thermoresponsive shape memory polymers. *Advanced Optical Materials* **3**, 1509-1516 (2015).

23 Jiang, P., Hwang, K. S., Mittleman, D. M., Bertone, J. F., & Colvin, V. L. Template-directed preparation of macroporous polymers with oriented and crystalline arrays of voids. *Journal of the American Chemical Society* **121**, 11630-11637 (1999).

BIOGRAPHICAL SKETCH

Rao Fei received his Bachelor of Science in chemistry from Peking University in 2012. He then began his graduate studies at University of Florida. His research area includes solid state chemistry, shape memory polymer, and nanoscale technologies.